# Effects of N-linked glycosylation on the creatine transporter

Nadine STRAUMANN, Alexandra WIND, Tina LEUENBERGER and Theo WALLIMANN[1]

From the Swiss Federal Institute of Technology, ETH Zürich, Institute of Cell Biology, ETH Hönggerberg, 8093 Zürich, Switzerland

The CRT (creatine transporter) is a member of the $Na^+$- and $Cl^-$-dependent neurotransmitter transporter family and is responsible for the import of creatine into cells, and thus is important for cellular energy metabolism. We established for CRT an expression system in HEK-293 cells that allowed biochemical, immunological and functional analysis of CRT wild-type and glycosylation-deficient mutants. Analysis of HA (haemagglutinin)-tagged CRT-NN (wild-type rat CRT with an HA-tag at the C-terminus) revealed several monomeric immunoreactive species with apparent molecular masses of 58, 48 and 43 kDa. The 58 kDa species was shown to be plasma-membrane-resident by $EndoH_f$ (endoglycosidase $H_f$) and PNGase F (peptide N-glycosidase F) treatments and represents fully glycosylated CRT, whereas the 48 kDa and 43 kDa species were glycosylation intermediates and non-glycosylated CRT respectively. Glycosylation-deficient mutants ($Asn^{192}Asp$, $Asn^{197}Asp$ and $Asn^{192}Asp/Asn^{197}Asp$) showed altered electrophoretic mobility, indicating that CRT is indeed N-glycosylated. In addition, a prominent CRT band in the range of 75–91 kDa was also detected. Pharmacological inhibition of N-linked glycosylation by tunicamycin in CRT-NN-expressing cells gave a similar reduction in molecular mass, corroborating the finding that $Asn^{192}$ and $Asn^{197}$ are major N-glycosylation sites in CRT. Although the apparent $K_m$ was not significantly affected in glycosylation-deficient mutants compared with CRT-NN, we measured reduced $V_{max}$ values for all mutants (21–28 % residual activity), and 51 % residual activity after enzymatic deglycosylation of surface proteins in intact CRT-NN cells by PNGase F. Moreover, immunocytochemical analysis of CRT-NN- and CRT-DD-expressing cells (where CRT-DD represents a non-glycosylated double mutant of CRT, i.e. $Asn^{192}Asp/Asn^{197}Asp$) showed a lower abundance of CRT-DD in the plasma membrane. Taken together, our results suggest that plasma-membrane CRT is glycosylated and has an apparent monomer molecular mass of 58 kDa. Furthermore, N-linked glycosylation is neither exclusively important for the function of CRT nor for surface trafficking, but affects both processes. These findings may have relevance for closely related neurotransmitter transporter family members.

Key words: cellular energetics, creatine transporter, creatine uptake, N-linked glycosylation, subcellular distribution.

## INTRODUCTION

Creatine and phosphocreatine are essential components of energy metabolism in tissues with high and fluctuating energy demands [1]. Transport of creatine from the bloodstream to tissues of creatine utilization is achieved by a 12-transmembrane-spanning transporter termed CRT (creatine transporter). CRT belongs to the superfamily of $Na^+$- and $Cl^-$-dependent neurotransmitter transporters, and is evolutionarily related the closest to the GABA ($\gamma$-aminobutyric acid) transporter [2,3]. Defects in the creatine synthesis pathway or mutations in the CRT gene located at the Xq28 locus lead to severe neurodegenerative and neuromuscular disorders [4,5], demonstrating the importance of CRT and creatine in health and disease. Nevertheless, attempts at the molecular and biochemical characterization of endogenous and recombinant CRT have proven frustrating so far, and have been complicated by the fact that the anti-CRT peptide antibodies prepared by Guerrero-Ontiveros and Wallimann [6] can cross-react with mitochondrial PDH (pyruvate dehydrogenase)-1 protein complexes [7] in crude lysates from tissues with high mitochondrial content. These antibodies were used for numerous studies, presenting a diversity of apparent molecular masses for CRT from several cell types and tissues [8–18]. Enrichment of the plasma membrane CRT by surface biotinylation of cardiomyocytes, or preparation of giant sarcolemma vesicles from skeletal muscle [11], as well as isolation of brush-border membranes [13] revealed one single immunoreactive polypeptide species each, with an apparent electrophoretic mobility of approx. 57–58 kDa, although the calculated molecular mass of CRT from its amino acid sequence would be approx. 70 kDa. In accordance with these findings, a 56 kDa CRT species was also described in red blood cells, which are devoid of mitochondria [16]. Other attempts by Dodd et al. [19] to enrich CRT by surface biotinylation of HEK-293 (human embryonic kidney-293) cells gave CRT immunoreactive signals at 90 kDa, whereas the same group recently reported the purification of CRT with an apparent molecular mass of 70 kDa [18]. Studies by other groups using different antibodies did not shed more light on the molecular identity of CRT, probably owing to the same inherent cross-reaction of anti-CRT antibodies with PDH [20–22]. Treatment of CRT-expressing cells with tunicamycin [21] or cell lysates with PNGase F (peptide N-glycosidase F) [18] indicated that CRT may be glycosylated, but the uncertainty about the apparent molecular mass of mature CRT remained.

For closely related family members of CRT, such as GABA transporter (GAT-1) [23], 5HTT [5-hydroxytryptamine (serotonin) transporter] [24], human NET [norepinephrine (noradrenalin) transporter] [25] and human DAT (dopamine transporter) [26], multiple protein species with different electrophoretic mobility encoded by one cDNA have also been observed. It was

Abbreviations used: CRT, creatine transporter; DAT, dopamine transporter; $EndoH_f$, endoglycosidase $H_f$; ER, endoplasmic reticulum; FCS, fetal bovine serum; GABA, $\gamma$-aminobutyric acid; GAT, GABA transporter; HA, haemagglutinin; HEK-293, human embryonic kidney-293; 5HTT, 5-hydroxytryptamine (serotonin) transporter; $\beta$-GPA, $\beta$-guanidinopropionic acid; LDS, lithium dodecyl sulphate; NET, norepinephrine (noradrenalin) transporter; PDH, pyruvate dehydrogenase; PNGase F, peptide N-glycosidase F; WGA, wheat-germ agglutinin.

[1] To whom correspondence should be addressed (email theo.wallimann@cell.biol.ethz.ch).

shown that the different species are generated by N-glycosylation of the large extracellular loop between transmembrane domains III and IV, a topological feature common to all members of this neurotransmitter transporter family. The positions of these N-glycosylation sequons are not conserved throughout all family members, but are all located at homologous positions within the extracellular loop II. A conspicuous feature in electrophoretic mobility of these highly hydrophobic 12-transmembrane-spanning protein family members is the persistent appearance of prominent higher molecular species, which are thought to display oligomeric, SDS-resistant forms of the transporters [23], whereas the monomeric forms all show an apparent molecular mass between 50 kDa and 60 kDa.

To our knowledge, no investigations have been carried out concerning the position of N-glycosylated residues in CRT and whether or how N-bound glycans could affect CRT function. For the 5HTT, Tate and Blakely [24] concluded that N-glycosylation is not essential for its uptake function (an unchanged $K_m$ for glycosylation-deficient mutants), but is essential for optimal stability (reduced $V_{max}$ for glycosylation-deficient mutants), biosynthetic maturation and functional expression, as predicted for many other glycoproteins [27–31]. Comparable studies with the same outcome were presented for the DAT [32], GAT [23,33] and NET [25,34,35]. However, in contradiction with Torres et al. [32], Li et al. [26] found for the DAT a dual role for N-bound glycans: first, for correct insertion in the plasma membrane, and secondly, for the function of the transporter.

The study presented here describes the expression, biochemical and functional characterization of rat CRT expressed in HEK-293 cells. We describe a novel approach to determine the apparent molecular mass of heterologously expressed CRT fused to an HA (haemagglutinin)-epitope tag by lithium-based denaturing gel electrophoresis. Furthermore, the glycosylation pattern of CRT is analysed; first, by using tunicamycin as a pharmacological inhibitor of N-glycosylation, and secondly, by site-directed mutagenesis of the canonical glycosylation sequons on CRT. The possible roles of N-linked glycosylation for surface trafficking and function are investigated and discussed.

## MATERIAL AND METHODS

### Eukaryotic cDNA expression constructs

The CRT cDNA (GenBank® accession number X66494) [36] was amplified by Expand High Fidelity polymerase (Roche) using primers 'CHOT1 for' (5′-AAAAGAATTCGCCATGGCGAAGAAGAGCGC-3′) and 'CHOT1 rev' (5′-AAAAGGATCCTGCCACATGACACTCTCCACC-3′) for the CRT-NN (wild-type rat CRT HA-tagged at the C-terminus) construct, and primers 'CHOT2 for' (5′-AAAAGAATTCGGCCATGGCGAAGAAGCG-3′) and 'CHOT2 rev' (5′-TTTGGATCCTCACATGACACTCTCC-3′) for the CRT-C-NN (wild-type CRT HA-tagged at the N-terminus) construct. This amplification step introduced new EcoRI and BamHI endonuclease restriction sites at the C- and N-termini of the CRT cDNA respectively. Samples (2 $\mu$g) of PCR products were digested with 40 units of EcoRI and BamHI (New England Biolabs), and then ligated (T4 DNA ligase; New England Biolabs) into expression plasmids pHAN1 (CRT-NN) and pHAC1 (CRT-C-NN) containing an HA-epitope tag at the C- and N-termini of the multiple cloning site respectively (see Figure 1A). pHAN1 and pHAC1 were derived from pEGFPN1 and pEGFPC1 (ClonTech) by replacing enhanced green fluorescent protein with HA [37]. All CRT inserts were fully sequenced.

### Mutation of glycosylation sequons by site-directed mutagenesis

Site-directed mutagenesis was used to mutate glycosylation sequons at positions $Asn^{192}$ and $Asn^{197}$ to $Asn^{192}$Asp (CRT-DN) and $Asn^{197}$Asp (CRT-ND) in CRT-NN cells. Primers '$Asn^{192}$Asp' (5′-GAAGACTGTGCCGATGCCAGCTTGG-3′) and '$Asn^{197}$Asp' (5′-CCAGCTTGGCCGACCTCACATGTG-3′) were used for the T7 DNA polymerase step, inserting an A-to-G mutation at required positions (see Figure 3B). The resulting mammalian expression constructs, CRT-DN and CRT-ND, were fully sequenced. For the generation of the double mutant ($Asn^{192}$Asp/$Asn^{197}$Asp) expression construct, CRT-DD, the two single mutant constructs were partially digested with 10 units of BglII for 5 min and re-ligated into the chimaeric CRT-DD construct containing both mutations (see Figure 1A).

### Cell cultures and heterologous expression of the CRT in HEK-293 cells

All experiments were performed in HEK-293 cells. They were cultured in DMEM (Dulbecco's modified Eagle's medium) containing 4.5 g/l glucose (Amimed), 10 % FCS (fetal bovine serum), 1 % (v/v) penicillin (10000 units/ml) 1 % (v/v) streptomycin (10000 $\mu$g/ml) and 2 mM L-glutamine under conditions of 6 % $CO_2$ and 95 % humidity at 37 °C. For transient transfection, $2 \times 10^5$ HEK-293 cells were plated in 35 mm dishes (Nuclon) coated with 0.1 % gelatine and grown for 24 h until 50 % confluence was attained, before transfection with 2 $\mu$g of DNA in 100 $\mu$l of OptiMEM and 3 $\mu$l of FuGENE™ (Roche). The transfection medium remained on the cultures until the cells were assayed.

### Cell lysis and protein separation techniques

At 24 h after transfection, cells were washed once with 1 × PBS and lysed in 10 $\mu$l of lysis buffer [1 % Triton X-100/60 mM Chaps/0.25 % deoxycholic acid/200 mM Tris/HCl (pH 8)/1 mM EDTA/1 mM EGTA/10 % (w/v) sucrose/Complete™ mini-protease inhibitor cocktail (Roche)]. Samples (8 $\mu$g) of cell lysate were analysed using the NuPAGE system (polyacrylamide 4–12 % Bistris gels) containing LDS (lithium dodecyl sulphate) sample buffer, antioxidant and Mops chamber buffer (Invitrogen). Separated proteins were transferred on to Protran nitrocellulose membranes (Schleicher and Schuell) by semi-dry Western blotting. Protran membranes were subsequently probed for 1 h with a 1:5000 dilution of M $\alpha$ HA antibody (Roche) or 1:5000 dilution of R $\alpha$ N-terminal CRT [6] antibody in TBS containing 0.1 % Tween 20 and 5 % skimmed milk powder. Secondary G $\alpha$ R-HRP antibodies (Calbiochem) were diluted 1:10000 in TBS containing 0.1 % Tween 20 and 5 % skimmed milk powder. The immunoreactive bands were visualized using the chemiluminescence detection kit (Axon Lab AG, Switzerland).

### Inhibition of N-linked glycosylation *in vivo*

Tunicamycin (5 $\mu$g/ml; Sigma) was added to HEK-293 cells simultaneously as they were transfected, and remained in the growth medium until the cells were assayed.

### EndoH$_f$ (endoglycosidase H$_f$) digestion

For removal of unprocessed N-glycans, 50 units of EndoH$_f$ (New England Biolabs), 1 $\mu$l of 10 × G7 buffer and 10 $\mu$g of cell lysate were combined in a final volume of 10 $\mu$l. The reaction mixture was incubated for 1 h at 37 °C.

### PNGase F digestion

For removal of all N-glycans *in vitro*, 500 units of PNGase F (New England Biolabs), 1 $\mu$l of 10 × G7 buffer and 10 $\mu$g of cell

lysate were combined in a final volume of 10 $\mu$l. The reaction mixture was incubated for 1 h at 37 °C. For removal of N-glycans displayed at the surface of intact HEK-293 cells, cells were washed twice with Hanks buffer (Amimed) and then incubated for 1 h with 200 $\mu$l of Hanks buffer containing 2000 units of PNGase F and 20 $\mu$l of 10 × G7 buffer (the protocol for 24-well plates). Cells were washed three times with Hanks buffer before the lysis procedure.

### [$^{14}$C]Creatine transport assays

HEK-293 cells ($7 \times 10^4$) were plated (24-well plates) 24 h before transfection, and grown until 50 % confluence was attained. Transfection was performed as described above. At 24 h after transfection, cells were serum-starved for 30 min at 37 °C in Hank's buffer, and then washed twice with KRH (Krebs–Ringer–Hepes) buffer [10 mM Hepes (pH 7.4)/4.7 mM KCl/2.2 mM $CaCl_2$/1.2 mM $MgSO_4$/1.2 mM $KH_2PO_4$/10 mM glucose] [38] containing either 120 mM NaCl or 120 mM LiCl. For [$^{14}$C]creatine-uptake time course assays, 250 $\mu$l of KRH/NaCl or KRH/LiCl containing 10 $\mu$M [$^{14}$C]creatine (0.14 $\mu$Ci; American Radiolabeled Chemicals Inc.) were added to the cultures and incubated for 15, 30, 60 or 90 min ($n = 6$ for each time point) at 37 °C. For kinetic assays, [$^{14}$C]creatine-uptake ratios were measured at concentrations of creatine of 1, 1.5, 3, 5, 10, 20, 50, 100 and 200 $\mu$M (0.001 $\mu$Ci/$\mu$M cold creatine) after 40 min. Creatine uptake was stopped by aspirating the uptake medium and washing the cells twice with 1 ml of ice-cold KRH/LiCl buffer. HEK-293 cells were solubilized with 200 $\mu$l of 0.5 % Triton X-100 and counted in 2 ml of scintillation cocktail Ultima Gold XR (Packard) in a Packard 1500 Tri-Carb liquid scintillation counter. Duplicate samples were also taken to determine protein concentrations using the detergent-compatible $D_c$ kit (Bio-Rad). Statistical analysis was performed using one-way ANOVA with a confidence interval of 95 %.

### Immunofluorescence and image analysis

For immunocytochemical analysis, HEK-293 cells were plated on to gelatin (0.1 % gelatin in $H_2O$) and fibronectin-coated glass slides, and transfected as described above. At 24 h after transfection, cells were washed twice with pre-warmed PBS, fixed at ambient temperature for 15 min with PFA (paraformaldehyde) solution (4 % PFA and 5 % sucrose in PBS) and permeabilized for 20 min with Triton solution (0.1 % Triton X-100 and 10 % FCS in PBS). The primary antibodies M $\alpha$ HA (Roche) and R $\alpha$ calnexin were diluted 1:5000 and 1:200 respectively in antibody incubation buffer (1 % FCS in 1 × PBS), and incubated for 1 h at ambient temperature. The secondary antibodies G $\alpha$ M-FITC (Cappel) and G $\alpha$ R-Cy3 (Jackson) were both diluted 1:400 in antibody incubation buffer and incubated for 1 h at ambient temperature. For mitochondrial staining, HEK-293 cell cultures were incubated with 100 $\mu$M Mitotracker Red MXRos (Molecular Probes) for 20 min at 37 °C and washed thoroughly with pre-warmed PBS before cell fixation. For plasma membrane staining with FITC-labelled WGA (wheat-germ agglutinin), 2 $\mu$g/$\mu$l FITC-WGA was added to the cells together with the secondary antibody. Stained cells were embedded in antifading medium [70 % (v/v) anhydrous glycerol/30 mM Tris/HCl (pH 9.5)/240 mM *N*-propyl gallate] and analysed microscopically using a Delta Vision Spectris Deconvolution system.

## RESULTS

### Expression of CRT in mammalian HEK-293 cells

Two different CRT expression constructs under the control of the CMV (cytomegalovirus) promoter were made. The constructs

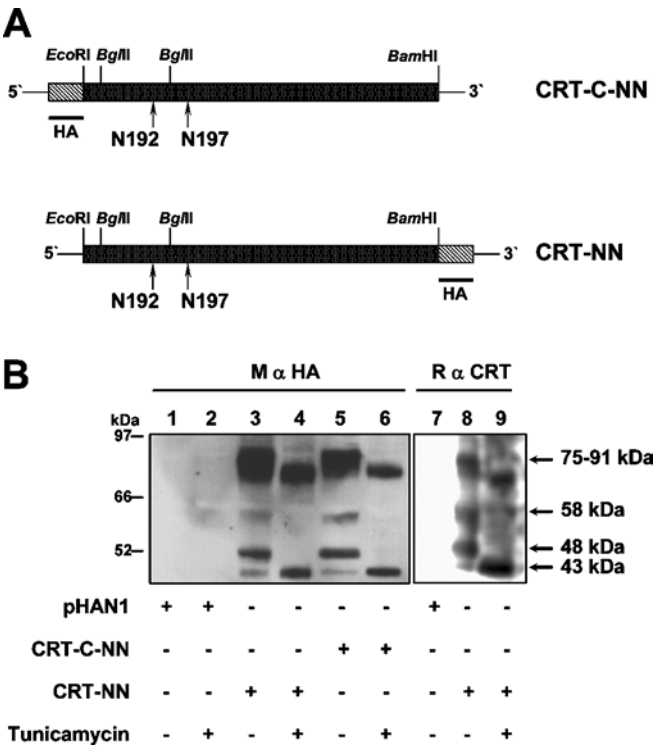


**Figure 1 CRT cDNA expressed in HEK-293 cells**

In (**A**) rat CRT cDNA (shaded box) was amplified by PCR and subcloned with EcoRI and BamHI into the plasmids pHAC1 (CRT-C-NN) and pHAN1 (CRT-NN) containing an HA-epitope tag (hatched box) at the N -and the C-termini respectively of the MCS (multiple cloning site). Amino acids $Asn^{192}$ and $Asn^{197}$ are canonical N-glycosylation sites within the extracellular loop II. (**B**) The expression pattern of CRT-NN and CRT-C-NN in HEK-293 cells was analysed in 8 $\mu$g of total protein lysate loaded on to LDS-PAGE. Immunoreactive species with apparent electrophoretic mobilities of 75–91, 58, 48 and 43 kDa were recognized by anti-HA and anti-CRT antibodies for CRT-NN and CRT-C-NN (lanes 3, 5 and 8) on a Western blot. No signal was seen in mock-transfected cells (lanes 1 and 7). Concomitant treatment of CRT-NN- and CRT-C-NN-expressing cells with tunicamycin (5 $\mu$g/ml) abolished the 58 and 48 kDa species, and led to a band shift of the 75–91 kDa region to 70–86 kDa (lanes 4, 6 and 9). The higher-molecular-mass region at 75–91 kDa is likely to represent a homodimeric form of CRT-NN and CRT-C-NN.

containing an HA-epitope tag at either the N-terminus (CRT-C-NN) or the C-terminus (CRT-NN) of CRT (Figure 1A) were expressed in HEK-293 cells. At 24 h post-transfection, cell lysates were analysed by NuPAGE Bistris PAGE (Invitrogen) followed by Western blotting. Prior attempts to separate HEK-293 cell lysates on Laemmli SDS/PAGE revealed unsatisfactory CRT signals on Western blots, probably owing to low protein resolution or aggregation of the highly hydrophobic CRT during sample preparation and extensive heating procedures (results not shown). Unlike in SDS/PAGE, protein separation in NuPAGE polyacrylamide gels is performed at neutral pH in the absence of SDS. This gel formulation prevents polyacrylamide hydrolysis, thus avoiding band distortion and loss of resolution. Moreover, the redox state within the gel is well controlled during electrophoresis, increasing band sharpness. The sample buffer is based on LDS instead of SDS that is normally used in Laemmli sample buffer, which allows protein denaturation and complete reduction of disulphides under mild conditions without extensive heating of the sample, which would lead to aggregation of membrane proteins. Although Western blots from SDS/PAGE gave a band pattern comparable with immunoblots from NuPAGE, the protein resolution was markedly increased with the NuPAGE system. Western blots probed with anti-HA antibody showed three

different forms for CRT-NN and CRT-C-NN at 58, 48 and 43 kDa (Figure 1B, lanes 3 and 5), all diverging substantially in their apparent molecular mass from the one predicted from the cDNA sequence (72 kDa). No signals were detected in mock-transfected cells (Figure 1B, lanes 1 and 2). A fourth immunoreactive high-molecular-mass region between 75–91 kDa, as seen for all other related family members of neurotransmitter transporters, was also observed for CRT-NN and CRT-C-NN. The higher-molecular-mass region between 75 and 91 kDa may have represented LDS-resistant homodimeric states of CRT. Such high-molecular-mass forms of $Na^+/Cl^-$-dependent neurotransmitter transporters have been described for many other family members, and are believed to display the functional multimeric transporter unit at the plasma membrane [32,39,40]. It may also be possible, however, that the high-molecular-mass species observed here represented overexpression artefacts due to unspecific aggregate formation of the hydrophobic protein, since in tissues with normal levels of CRT no such higher-molecular-mass region could be observed [11,13,16].

Two possibilities could explain the discrepancy of apparent mass from the predicted molecular mass for the bands at 58, 48 and 43 kDa: either the transporter was proteolytically degraded during sample preparation, or the bands represented different glycosylation states of CRT. Proteolytic degradation could be excluded, since no differences in the Western blot could be found between CRT-C-NN and CRT-NN, containing the HA-tag at opposing termini (Figure 1B, lanes 3 and 5). Moreover, computational analysis revealed an asymmetrical distribution of possible protease cleavage sites within the primary CRT sequence; hence an asymmetrical band pattern would be expected for the constructs containing the HA-tag at different locations. To corroborate these findings, the same CRT-NN cell lysate was probed with anti-N-terminal CRT peptide antiserum generated by Guerrero-Ontiveros and Wallimann [6], which gave again the same band pattern on a Western blot (Figure 1B, lane 8). The specificity of this antiserum for CRT was tested on mock-transfected HEK-293 cells, where no signals were detectable (Figure 1B, lane 7). Notably, as compared with skeletal muscle and heart, no cross-reactivity with mitochondrial PDH at 55 and 70 kDa could be observed, probably due to the high concentration of CRT-NN compared with the rather low content of mitochondria in HEK-293 cells. Thus the anti-N-terminal CRT peptide antiserum from Guerrero-Ontiveros and Wallimann [6] gave trustworthy results in lysates with a high CRT to total protein ratio and a low mitochondrial content. However, the unspecific background of this antibody remained very high, and could not be improved either by increased stringency of the antibody-binding solution or by prolonged washing procedures. This was probably due to the fact that the antiserum was not affinity-purified. From these data, we concluded that the anomalous migration of the CRT transporter on denaturing PAGE was an intrinsic characteristic of this highly hydrophobic 12-transmembrane-spanning protein. A comparable anomalous migration was reported for heterologously expressed GFP-tagged [41] and untagged [26] DAT, GAT [23], NET [35] and 5HTT [24]. Moreover, several groups reported a genuine CRT with an apparent molecular mass of 56–58 kDa in enriched plasma membrane fractions [11,13,16,17], which is concordant with the migration behaviour we reported here for the HA-tagged version of CRT. We therefore exclude the possibility that the HA-tag affects electrophoretic behaviour of CRT-NN.

CRT-NN and CRT-C-NN showed the same expression levels in HEK-293 cells as quantified on Western blots. Therefore all further experiments were performed with CRT-NN-expressing HEK-293 cells, where the HA-tag was expressed at the C-terminus of CRT.

Furthermore, we were interested in the subcellular distribution of heterologously expressed CRT-NN. Immunofluorescence analysis with anti-HA antibody revealed an intracellular reticular pattern of CRT-NN, as well as a peripheral signal (Figures 2A, 2E and 2H). Co-staining with the ER (endoplasmic reticulum) marker protein calnexin (Figure 2C), the mitochondrial marker Mitotracker (Figure 2F) and the FITC-labelled lectin WGA (Figure 2H) revealed a co-localization of CRT-NN with calnexin signals (Figure 2D), plasma-membrane-resident WGA signals (Figure 2J), and, in contradiction with former studies [12], no co-localization of CRT-NN with the mitochondrial compartment could be seen (Figure 2G). Since FITC-labelled WGA was added to the permeabilized cells, a strong intracellular WGA signal in the Golgi compartment that did not co-localize with CRT-NN could be detected too (Figure 2J). The strong retention of expressed CRT-NN in the ER might be attributed to the presence of the HA-tag, but could also be due to the high amount of CRT-NN of the normally only lowly abundant CRT. Mock-transfected cells showed no unspecific immunofluorescence signal (Figure 2B).

### Presence of N-glycosylation in the CRT

The cDNA of CRT predicts two canonical N-glycosylation sites located within the extracellular loop between transmembrane domains II and III at positions $Asn^{192}$ and $Asn^{197}$ (Figures 1A and 3A). Although the occurrence of these predicted sites within the extracellular loop II is common to all members of the neurotransmitter transporter family, the positions of the glycosylation sites are not conserved throughout the entire family. Sequence alignments of rat and human CRT with GAT and 5HTT showed that the CRT glycosylation sequon located at $Asn^{197}$ is conserved throughout the monoamine and $\gamma$-aminobutyric acid transporter family, whereas the sequon at $Asn^{192}$ is not (Figure 3A).

As shown in Figure 1(B), HEK-293 cells expressing CRT-NN or CRT-C-NN displayed four anti-HA immunoreactive bands on a Western blot. In a pharmacological approach, transfected HEK-293 cells were incubated with the strong N-glycosylation inhibitor tunicamycin. This treatment abolished the immunoreactive species running at 58 and 48 kDa and was paralleled by an increase in intensity of the 43 kDa species. The high-molecular-mass region at 75–91 kDa shifted down to 70–86 kDa following tunicamycin treatment.

To investigate further the exact position and function of N-glycosylation, and to circumvent the disadvantageous apoptotic side effects of tunicamycin, three different site-directed mutants of CRT-NN were constructed that were lacking the N-glycosylation sequons. The asparagine residues at $Asn^{192}$ and $Asn^{197}$ were sequentially replaced by an aspartate residue, leading to the $Asn^{192}$Asp (CRT-DN) and $Asn^{197}$Asp (CRT-ND) single mutants and the $Asn^{192}$Asp/$Asn^{197}$Asp (CRT-DD) double mutant (Figure 3B). Wild-type CRT-NN and mutated CRT-ND, CRT-DN and CRT-DD were expressed in HEK-293 cells either with or without tunicamycin administration. Immunoblots of these total cell homogenates with anti-HA antibody showed for CRT-NN + tunicamycin, CRT-DD and CRT-DD + tunicamycin the above-described non-glycosylated CRT core protein running at an apparent molecular mass of 43 kDa (Figure 3C, lanes 4, 5 and 6 respectively). This indicated that: (i) CRT contained N-glycosylated residues; and (ii) $Asn^{192}$ and $Asn^{197}$ are the major glycosylation sites on CRT. For the single mutants, CRT-ND and CRT-DN, the situation was slightly different: the 58 kDa species of CRT-NN containing two N-linked sugars was shifted down to 51 kDa for the mutants containing only one sugar, and the predominant 48 kDa species was shifted to 46 kDa (Figure 3C, lanes 7 and 9 respectively). After tunicamycin treatment of

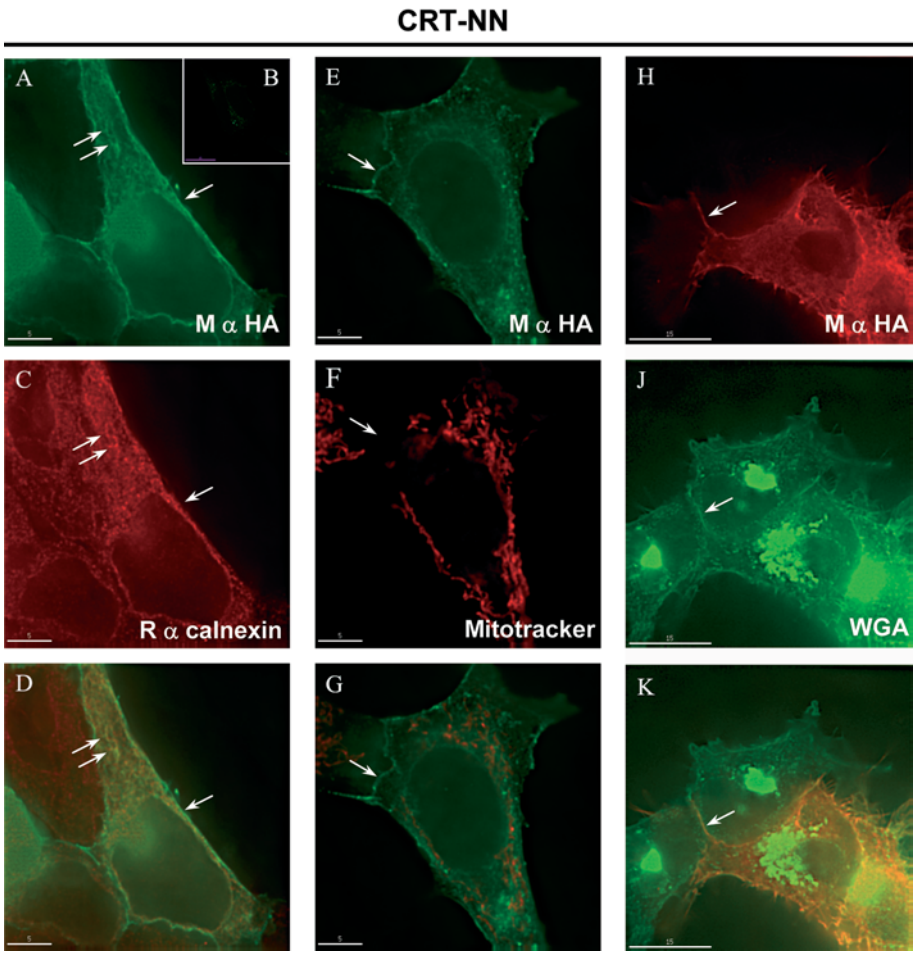


**Figure 2 Subcellular distribution of wild-type CRT-NN**

In immunocytochemical assays, HEK293 cells expressing CRT-NN were probed with anti-HA (green), anti-calnexin (panels **C** and **D**, red) or Mitotracker (panels **F** and **G**, red). Plasma membrane was visualized using FITC-labelled wheat germ agglutinin WGA (panel **J** and **K**, green). The CRT-NN signal (**A**, **E** and **H**) revealed a reticular distribution of CRT-NN that co-localized with the calnexin staining (**A**, **C** and **D**, double arrows). The CRT-NN signal was also detectable at the plasma membrane and in cellular boundaries (**J** and **K**, arrows). The Mitotracker signal (**F**) showed no overlap with CRT-NN immunofluorescence (**G**). Mock-transfected HEK293 cells showed no staining (**B**). Scale bar A-G: 5 $\mu$m. Scale bar H–K: 15 $\mu$m.

these mutants, only the core protein at 43 kDa remained detectable (Figure 3C, lanes 8 and 10 respectively). Blockage of N-glycosylation by tunicamycin or deletion of glycosylation sites did not impair the total expression levels of CRT-NN, CRT-DN, CRT-ND and CRT-DD, as estimated by densitometric measurements of the Western blotting data. These results suggested a monomeric non-glycosylated CRT core protein with an apparent electrophoretic mobility of 43 kDa, a partially glycosylated form of CRT of 48 kDa and a fully glycosylated mature CRT of 58 kDa.

Immunocytochemical analysis of the generated mutants CRT-ND, CRT-DN and CRT-DD revealed a comparable reticular pattern to that described for CRT-NN (Figure 4). Whilst a weak plasma membrane signal could still be detected in few cells for the CRT-DN mutant (Figure 4B, panels I), no comparable staining was visible for the CRT-ND (Figure 4A, panels I and IV) and CRT-DD mutants (Figure 4C, panels I, IV and VII), associated with an increase in the intracellular retention of the mutated transporter. Merging the anti-HA and the anti-calnexin staining for CRT-DN (Figure 4B, panel III), CRT-ND (Figure 4A, panel III) and CRT-DD (Figure 4C, panel III)-expressing HEK-293 cells revealed that the majority of overexpressed protein co-localized with the ER. For CRT-DD, no plasma-resident signal that co-localized with WGA-FITC could be detected (Figure 4C, panel IX). Co-localization with mitochondria could again be excluded (Figures 4A, 4B and 4C, panels V and VI). Hence deletion of one or both glycosylation sequons largely abolished the plasma membrane signal, indicating the possibility that partially glycosylated or non-glycosylated CRT was not exported from the ER and targeted to the plasma membrane as successfully as the fully glycosylated CRT. CRT-NN-expressing cells treated with tunicamycin showed no plasma membrane staining either, corroborating the findings described above (results not shown).

### Identification of the functional plasma membrane form of CRT

Two approaches were chosen to identify the fully glycosylated, plasma-membrane-resident forms of CRT on Western blots. In our first approach, HEK-293 cell lysates were treated with $EndoH_f$, which removes unprocessed core oligosaccharides. Glycoproteins, which contain a processed complex oligosaccharide, are resistant to $EndoH_f$ treatment and therefore are most probably plasma-membrane-resident. Digestion of CRT-NN cell extracts revealed an $EndoH_f$-resistant 58 kDa form of CRT-NN (Figure 5A, lanes 1 and 3). The 48 kDa species was completely digested by $EndoH_f$, therefore displaying an N-glycosylation

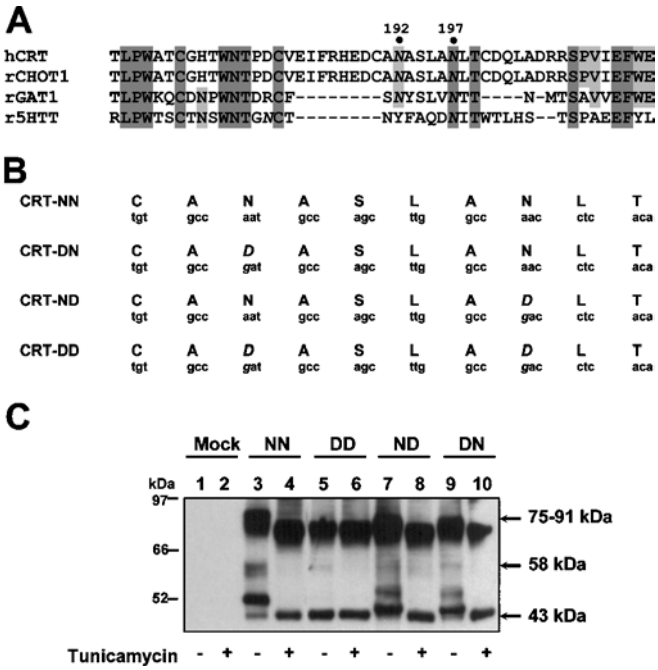


**Figure 3 Canonical N-glycosylation sites in CRT and removal of N-glycosylation sequons in CRT-NN by site-directed mutagenesis**

In (**A**) the human and rat CRT protein sequence was aligned with rat GAT1 and rat 5HTT. Canonical N-glycosylation sequons (shown in italics) lay within the large extracellular loop II. Amino acid $Asn^{197}$ is conserved throughout the family of monoamine and $\gamma$-aminobutyric acid neurotransmitter transporters, whereas $Asn^{192}$ is not conserved. High consensus is denoted by dark grey shading; low consensus is shown as light grey. (**B**) Canonical N-glycosylation sequons at positions $Asn^{192}$ and $Asn^{197}$ were removed in CRT-NN by site-directed mutation of A to G. Two single mutants (CRT-ND and CRT-DN) deficient in one canonical N-glycosylation sequon and one double mutant (CRT-DD) deficient in both glycosylation sequons were generated. (**C**) Lysates of HEK-293 cells expressing pHAN1, CRT-NN, CRT-DD, CRT-ND and CRT-DN respectively were analysed on a Western blot with anti-HA antibody. For CRT-NN, administration of tunicamycin (5 $\mu$g/ml) abolished the 58 and 48 kDa species and increased the amount of the 43 kDa species (lanes 3 and 4). For CRT-DD, only the 43 kDa was detectable in lysates with (lane 6) or without (lane 5) tunicamycin administration. For CRT-ND and CRT-DN, the 58 kDa band was shifted to 51 kDa and the 48 kDa band to 46 kDa (lanes 7 and 9 respectively); tunicamycin abolished all species except for the 43 kDa core-protein (lanes 8 and 10).

intermediate that was not yet fully processed and thus not located at the cell surface. The same $EndoH_f$ treatment was used for CRT-ND and CRT-DN to identify the 51 kDa band as being the fully glycosylated, $EndoH_f$-resistant form (Figure 5A, lanes 5 and 6 respectively).

These findings were confirmed in a second approach by *in vivo* deglycosylation of CRT-NN-expressing HEK-293 cells with PNGase F administrated to intact cells. In contrast with $EndoH_f$, PNGase F is known to deglycosylate both processed and unprocessed oligosaccharides. Glycans of intact cells facing the extracellular space were expected to be digested by PNGase F, leading to a lowered molecular mass of plasma-membrane-resident glycoproteins. As shown in immunoblots (Figure 5B, lanes 1 and 2), only the plasma-membrane-resident 58 kDa species of CRT-NN was deglycosylated by PNGase F added to the growth medium, leading to a shift in apparent molecular mass from 58 to 43 kDa. Hence, the fully glycosylated form of CRT-NN was present at the cell surface and showed an apparent molecular mass of 58 kDa. To show that the 48 kDa species could be digested if it were accessible to PNGase F, a lysate of CRT-NN-expressing HEK-293 cells was treated with PNGase F, which abolished the 58 kDa and 48 kDa immunoreactive bands (Figure 5B, lane 3). Thus only the 58 kDa species was present at the plasma membrane.

The broad higher-molecular-mass species of 75–91 kDa of CRT-NN also showed a down-shift in electrophoretic mobility after PNGase F treatment, thus indicating that a certain proportion of this CRT species, probably representing glycosylated dimers, is indeed also present at the plasma membrane.

### Functional analysis of heterologous wild-type CRT

The kinetics of [$^{14}$C]creatine uptake of CRT-NN-expressing cells were investigated. Uptake of creatine as a function of time showed a short lag phase, followed by a 50 min linear uptake phase that reached a plateau after 60 min (Figure 6A). The lag phase was probably due to the absence of a uniform mixing of [$^{14}$C]creatine added to the reaction mixture. The creatine-uptake experiment showed that expressed CRT-NN was present in the plasma membrane, and folded in a correct and active conformation to bind and transport creatine across the plasma membrane of intact cells. A rough estimation of $V_{max}$ values derived from the linear phase of [$^{14}$C]creatine uptake revealed for CRT-NN-expressing cells an approx. 13-fold increase in $V_{max}$ as compared with mock-expressing cells, indicating a higher density of heterologously expressed transporter at the cellular surface.

CRT co-transports creatine and sodium ions from the extracellular fluid, and therefore strongly depends on a physiological amount of sodium cations in the assay medium. Similar kinetic experiments were thus performed in parallel in NaCl- or LiCl-containing KRH buffer. The absence of $Na^+$ ions completely stopped creatine import, demonstrating the sodium-dependency of expressed CRT-NN and endogenous CRT (Figure 6B). To show specificity of CRT-NN for creatine, a 10-fold excess of the creatine analogue $\beta$-GPA ($\beta$-guanidinopropionic acid) over creatine was added to the reaction mixture after 30 min of normal uptake (Figure 6C). $\beta$-GPA successfully competed with [$^{14}$C]creatine for receptor binding and was transported by CRT-NN. Hence intracellular levels of [$^{14}$C]creatine no longer increased. The reported 13-fold increase in creatine uptake for CRT-NN, its sodium-dependency and the ability to compete creatine uptake with $\beta$-GPA indicated that the HA-tag did not affect the function and activity of CRT-NN. Furthermore, a recent study by Dodd and Christie [42] convincingly showed that only the third transmembrane domain of CRT is involved in the substrate pathway.

To assess the kinetic parameters, [$^{14}$C]creatine uptake was measured as a function of variable substrate concentrations for CRT-NN after 40 min of uptake (linear phase). The [$^{14}$C]creatine uptake followed saturation kinetics and was fitted using the Michaelis–Menten model. The apparent Michaelis–Menten constant ($K_m$) and maximal velocity ($V_{max}$) were determined by a massed Hanes–Woolf linearization (Figure 7, inset) of the primary kinetic data (Figure 7). In our HEK-293 cell system, an apparent $K_m$ of $37.3 \pm 6.8$ $\mu$M and a $V_{max}$ of $467.7 \pm 49.2$ pmol/mg per min were measured for wild-type CRT-NN.

### *N*-linked glycosylation of CRT is not absolutely required for [$^{14}$C]creatine transport

Furthermore, we were interested to answer the question as to whether and how N-glycosylation affected CRT function. Wild-type CRT-NN and glycosylation mutants CRT-ND, CRT-DN and CRT-DD were expressed in HEK-293 cells and [$^{14}$C]creatine transport kinetics were assessed at different substrate concentrations after 40 min of incubation. Each measurement was carried out independently, with four replicates each. The apparent $K_m$ values for CRT-ND, CRT-DN and CRT-DD revealed a non-significant decrease in $K_m$ upon mutation of a single or both

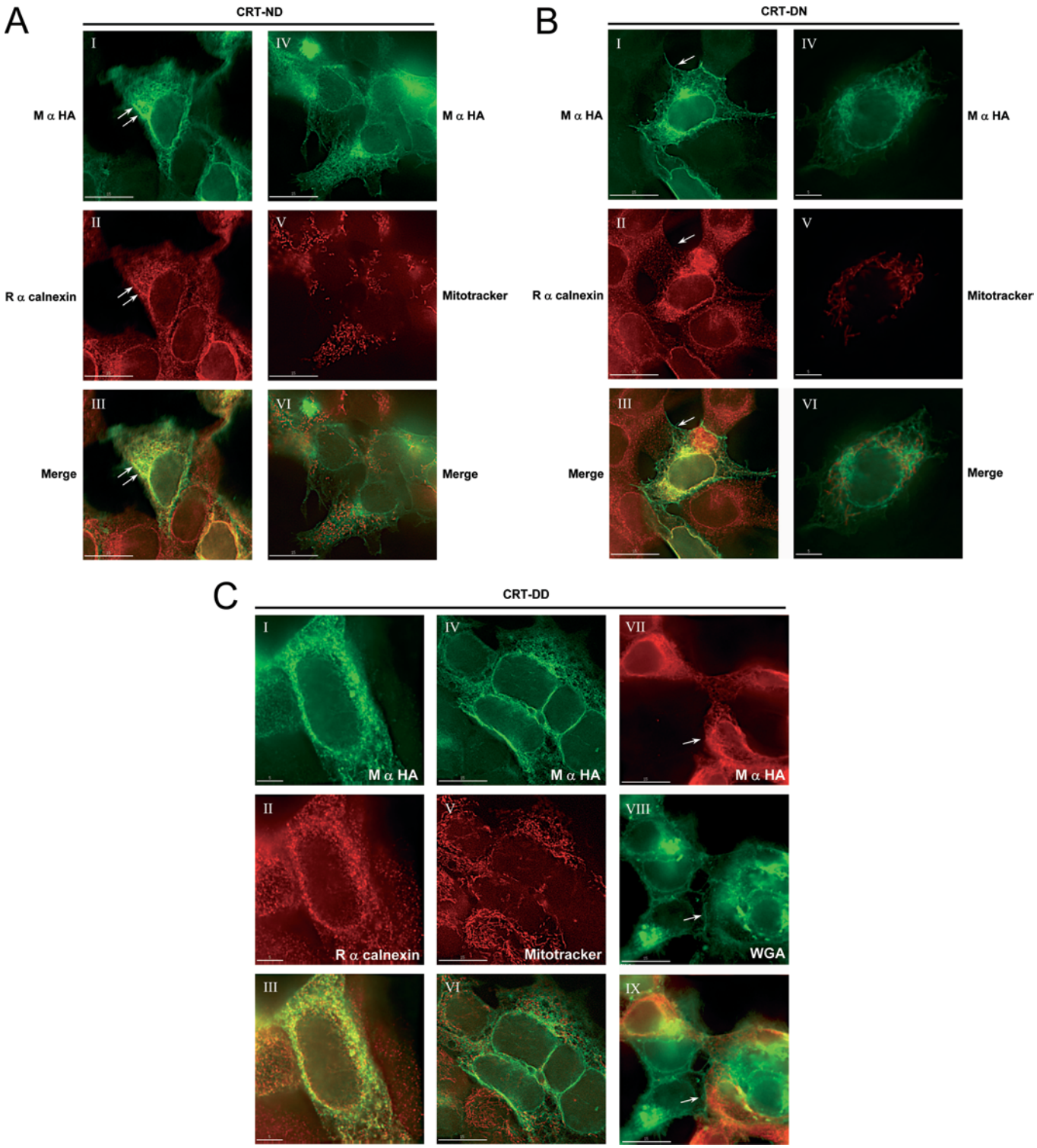


**Figure 4 Altered subcellular distribution after mutation of N-glycosylation sites**

Expression of glycosylation-deficient mutants CRT-ND (**A**), CRT-DN (**B**) and CRT-DD (**C**) revealed altered subcellular distribution of the mutants. The reticular CRT immunofluorescence (panels I and IV, green) co-localized (panel III) with the ER-resident calnexin staining (panel II, red), but not with the mitochondrial Mitotracker signal (panels V and VI, red). For CRT-DD (**C**) and CRT-ND, no plasma-membrane-resident staining could be detected (**C**, panels VII–IX, arrows). For CRT-DN, a few cells showed weak immunofluorescence at the cell boundaries (**B**, panel I). (**A**) Double arrows in panels I–III indicate reticular staining. (**B**) Single arrows in panels I–III indicate plasma membrane staining.

glycosylation sites ($P > 0.05$) (Table 1). The same observation could be made for CRT-NN-expressing cells that were treated with PNGase F to remove all glycans from plasma membrane CRT-NN prior to kinetic measurements. These results indicate that elimination of glycans from CRT slightly increased the substrate binding affinity of CRT for creatine.

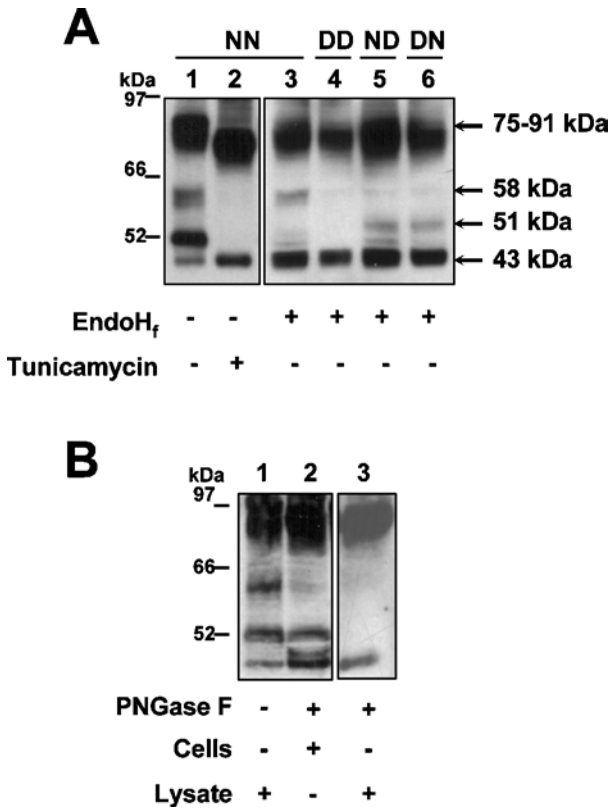


**Figure 5 Plasma-membrane-resident CRT-NN monomer has an apparent molecular mass of 58 kDa**

In (**A**) enzymatic deglycosylation of unprocessed glycans was performed with EndoH$_f$ (50 units/10 $\mu$g od protein) in HEK-293 cell lysates *in vitro*. For CRT-NN (NN), the 48 kDa species was deglycosylated, leading to an electrophoretic shift of 5 kDa (lane 3). The 58 kDa species was protected against EndoH$_f$ digestion. For CRT-DD (DD), no changes in band pattern were observed upon deglycosylation (lane 4). For CRT-ND (ND) and CRT-DN (DN), the 51 kDa band was protected against EndoH$_f$ (lanes 5 and 6 respectively). (**B**) Enzymatic deglycosylation of all glycans facing the extracellular space was achieved by addition of PNGase F (10 units/$\mu$l) to CRT-NN-expressing cells *in vivo*. Cleavage of all surface glycans *in vivo* produced a non-glycosylated plasma-membrane-resident CRT-NN with an electrophoretic mobility of 43 kDa (lane 2). As a control, total lysate was incubated *in vitro* with PNGase F, which showed deglycosylation of the 48 kDa species when accessible to PNGase F (lane 3). Corresponding effects could be observed for the higher-molecular-mass region.

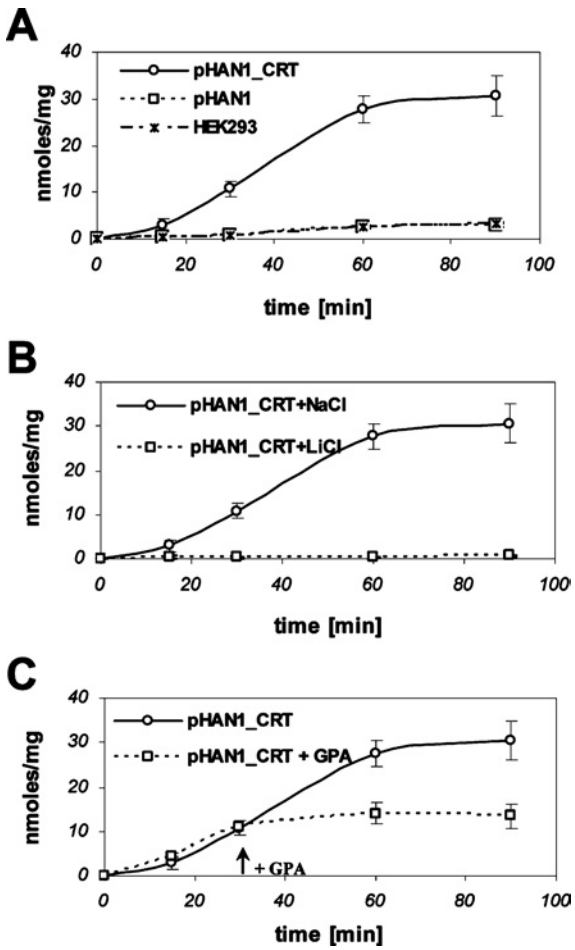


**Figure 6 Time-course of [$^{14}$C]creatine uptake into CRT-NN-expressing HEK293 cells**

Uptake of 10 $\mu$M [$^{14}$C]creatine (0.14 $\mu$Ci) was measured at 15, 30, 60 and 90 min. The amount of creatine uptake was expressed as nmol/mg per min, and values were the means $\pm$ S.D. for six independent experiments. (**A**) [$^{14}$C]Creatine import in HEK-293 cells expressing CRT-NN (○), pHAN1 (□) or in wild-type HEK293 cells (*) showed a 10 min lag-phase followed by a linear uptake phase of 50 min, before reaching a plateau after 60 min. From the slopes of the linear phase, an approx. 13-fold increase in CRT density at the plasma membrane of CRT-NN-expressing cells compared with wild-type or mock-transfected cells could be calculated. (**B**) $Na^+$-dependence of CRT-NN expressed in HEK-293 cells was shown using either NaCl- (○) or LiCl (□)-containing assay buffer. LiCl-containing buffer blunted [$^{14}$C]creatine uptake and lowered uptake rates below wild-type levels. (**C**) [$^{14}$C]Creatine uptake was competed by adding a 10-fold excess of $\beta$-GPA over creatine to the assay mix after 30 min of normal uptake (□). Intracellular [$^{14}$C]creatine levels remained therefore constant until the end of the measurements.

$V_{max}$ is a measure of the CRT transport activity at substrate saturation. In contrast with $K_m$, however, it is also dependent on the amount of CRT molecules at the cell surface. $V_{max}$ was reduced significantly ($P < 0.001$) in cells expressing the glycosylation-deficient mutants CRT-ND, CRT-DN and CRT-DD as compared with wild-type CRT-NN (Table 1). To determine whether this reduction in $V_{max}$ was due to impaired transport activity of the glycosylation-deficient mutants or to lower abundance of the transporter at the surface, functional activity of intact CRT-NN cells that were deglycosylated with PNGase F before the uptake assay was measured. A significantly impaired $V_{max}$ for deglycosylated CRT-NN cells as compared with untreated CRT-NN cells was noticed ($241.1 \pm 15.5$ and $467.7 \pm 49.2$ pmol/mg per min respectively; $P < 0.001$). This corresponded to a reduction of transport activity by 49%. If N-glycosylation were only essential for CRT transport activity, the same functional impairment would be expected for glycosylation-deficient mutants as for enzymatically deglycosylated CRT-NN. This was indeed true, but the transport activities were reduced further in cells expressing CRT-ND, CRT-DN and CRT-DD glycosylation mutants to 28%, 23% and 21% respectively of residual wild-type activity, indicating a lower abundance of mutated transporter at the cell surface. This was corroborated by the fact that non-glycosylated CRT was shown to be less abundant at the plasma membrane, as demonstrated by immunofluorescence (Figures 4A, 4B and 4C). Densitometric estimation of the CRT-NN 58 kDa and the single-mutant 51 kDa immunoreactive bands in Figure 3(C) gave an approx. 2–3-fold reduction in signal intensity for both plasma-membrane-resident CRT forms. Hence we concluded that N-linked glycosylation of both sites, Asn$^{192}$ and Asn$^{197}$, was also required for efficient targeting of CRT to the plasma membrane. Moreover, non-glycosylated or partially glycosylated CRT that reached the plasma membrane, or fully glycosylated CRT that was *in vivo* deglycosylated by PNGase F, showed impairments in functional activity.

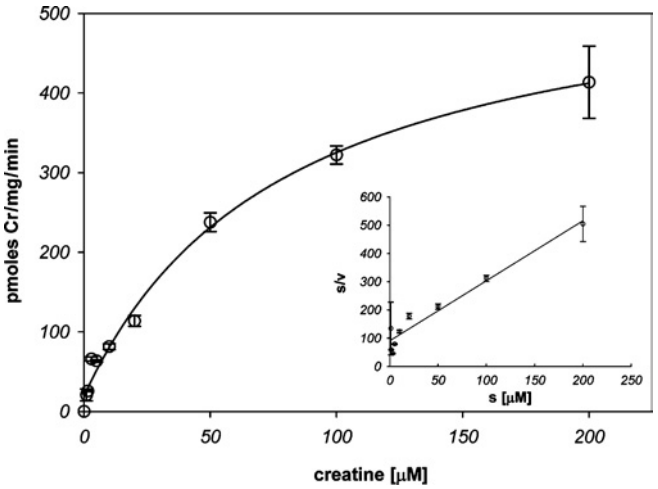


**Figure 7 Kinetics of [$^{14}$C]Creatine uptake in CRT-NN expressing HEK293 cells**

[$^{14}$C]Creatine uptake was measured as a function of variable creatine substrate concentrations (1, 1.5, 3, 5, 10, 20, 50, 100 and 200 $\mu$M) containing 0.001 $\mu$Ci [$^{14}$C]creatine per $\mu$M creatine within the linear phase (40 min). The velocity ($v$) of creatine uptake was expressed as pmol/mg per min, and values were means $\pm$ S.E.M. for four independent experiments. The velocity as a function of substrate concentration followed the Michaelis–Menten model. In the inset to the main Figure, the uptake curve was linearized with the weighted Hanes-Woolf algorithm (substrate concentration [S]/velocity ($v$) plotted against [S]). The apparent Michaelis–Menten constant ($K_m$) and maximal velocity ($V_{max}$) were 37.3 $\pm$ 6.8 $\mu$M and 467.7 $\pm$ 49.2 pmol/mg per min respectively.

**Table 1 $K_m$ and $V_{max}$ determinations for CRT and CRT glycosylation mutants in HEK-293 cells**

For [$^{14}$C]creatine uptake, CRT-NN-, CRT-ND-, CRT-DN- and CRT-DD-expressing cells were serum-starved before kinetic measurements. Cells were incubated with [$^{14}$C]creatine in KRH buffer for 40 min (linear phase). Results are the means $\pm$ S.E.M. for four experiments performed independently. See Figure 3(B) for nomenclature regarding CRT-NN and its mutants.

| Recombinant CRT | $K_m$* ($\mu$M) | $V_{max}$* (pmol creatine/mg per min) |
|---|---|---|
| CRT-NN | 37.3 $\pm$ 6.8 | 467.7 $\pm$ 49.2 |
| CRT-NN + PNGase F | 22.2 $\pm$ 2.5 | 241.1 $\pm$ 15.5† |
| CRT-ND | 24.2 $\pm$ 10.2 | 132.3 $\pm$ 14.4† |
| CRT-DN | 17.3 $\pm$ 3.6 | 108.2 $\pm$ 10.9† |
| CRT-DD | 20.6 $\pm$ 2.1 | 102.3 $\pm$ 6.6† |

* Values represent independent experiments, and errors are given as S.E.M. ($n = 4$).

† Statistical relevance was assessed using one-way ANOVA with an interval of confidence of 95 %, and gave $P < 0.001$.

## DISCUSSION

The aim of the work presented here was to characterize the molecular identity of the creatine transporter and to investigate the role of N-glycosylated residues in CRT. Determination of the apparent molecular mass of CRT on Western blots did not seem to be trivial up to now, since most CRT antibodies are known to cross-react with mitochondrial PDH [7], especially if used with crude cell or tissue lysates, or with enriched mitochondrial fractions. Our system using HA-tagged CRT does not depend on anti-CRT antibodies, but relies on specific anti-HA antibodies. As shown by immunoblotting data, the two canonical glycosylation sites at Asn$^{192}$ and Asn$^{197}$ are both used for sugar attachment to heterologously expressed rat CRT, because the three detected species of CRT-NN at 58, 48 and 43 kDa were reduced to one single non-glycosylated 43 kDa core protein after: (i) tunicamycin administration to the cells; (ii) CRT-NN lysates were enzymatically deglycosylated with PNGase F; or (iii) the two glycosylation sites at Asn$^{192}$ and Asn$^{197}$ were removed by site-directed mutagenesis (CRT-DD). Stepwise mutation of Asn$^{192}$ and Asn$^{197}$ led to intermediate forms that suggested an approx. 7–8 kDa impact for each glycosylated site of CRT. We identified further the 58 kDa species of CRT-NN as the only EndoH$_f$-resistant form that could also be deglycosylated by PNGase F added to intact cells. Hence the species with an apparent molecular mass of 58 kDa corresponds to the CRT monomer located at the plasma membrane. Analysing CRT-NN cell extracts with the anti-N-terminal CRT peptide antibody generated by Guerrero-Ontiveros and Wallimann [6], we asserted the same immunoreactive bands as seen with the anti-HA antibody. Hence this antibody cross-reacted only with PDH in extracts containing a high mitochondria to plasma membrane ratio. This new understanding may have implications for a number of studies, which were based on these antibodies and used crude cell lysates or enriched mitochondrial fractions [8–10,12,14–16]. However, experimental data from different authors obtained with enriched plasma membrane fractions clearly identified one endogenous CRT species with an apparent molecular mass of 56–58 kDa when using the same antibody [11,13,16,17], which was concordant with our 58 kDa plasma resident species presented here. In addition, immunocytochemical analysis of the subcellular distribution of CRT-NN showed no co-localization with the mitochondrial compartment, corroborating the findings of Speer et al. [7] that the formerly postulated mitochondrial CRT isoform [11,12] does not correspond to a genuine CRT.

The higher HA-immunoreactive molecular mass region between 75 and 91 kDa detected may display LDS-resistant dimeric forms of CRT with different glycosylation states. Oligomerization and the presence of SDS-resistant oligomers in heterologous expression systems have been described for GAT [23], NET [25] and 5HTT [39]. A recent study by West et al. [18] identified an apparent molecular mass for CRT of 210 kDa by gel filtration and 70–80 kDa on SDS polyacrylamide gels. They assume that the 210 kDa species corresponds to a dimeric form of CRT, which would support our findings. In this respect, the 70 kDa species reported by West et al. [18] might correspond to the higher-molecular-mass region at 75–91 kDa described here, thus representing an SDS- or LDS-resistant insoluble form of CRT.

The present results on creatine-uptake characteristics for plasma-membrane-resident wildtype CRT-NN gave an apparent $K_m$ of 37.3 $\pm$ 6.8 $\mu$M, which was within the range of formerly published values. Studies with endogenous CRT measured $K_m$ values of between 15 and 53 $\mu$M [11,13,43,44]. Transient and stable expression of different CRT cDNAs in HEK-293, Cos-7 and HeLa cells, as well as in *Xenopus* oocytes, confirmed the values found for endogenous CRT [21,36,45–48]. In contradiction with these results, Dodd and co-workers [19,22] reported not only a much higher $K_m$ for stable and transient expression of bovine CRT in HEK-293 cells, but also a markedly increased $V_{max}$. The reasons for these differences are not readily apparent. In contrast with our data presented here and the work performed with rat CRT cDNA expressed in HEK-293 cells by Schloss et al. [47], Dodd and co-workers 19,22] used bovine CRT cDNA, which has an overall identity of 89 % with the rat CRT cDNA.

Removal of one or both glycosylation sites at positions Asn$^{192}$ and Asn$^{197}$ resulted in a non-significant reduction in the apparent $K_m$ for all mutants. The same experiment performed with CRT-NN-expressing cells, which were enzymatically deglycosylated with PNGase F, confirmed this reduced value for $K_m$. Since Asn$^{192}$ and Asn$^{197}$ are in close proximity to Cys$^{144}$, which has been reported to play a crucial role in creatine substrate binding [22], it

is likely that the interaction between the second extracellular loop containing the glycosylation sequons and the third transmembrane domain being responsible for substrate recognition are facilitated after deglycosylation. The present findings of a slightly lowered $K_m$ are in accordance with kinetic measurements of comparable glycosylation mutants of the DAT [26] and the NET [35].

Major effects, however, were observed in $V_{max}$ for partially or non-glycosylated CRT. Upon mutation of one or both glycosylation sites, the apparent $V_{max}$ was significantly reduced by 72 %, 77 % and 79 % for the glycosylation mutants CRT-ND, CRT-DN and CRT-DD, respectively. This monitors either the importance of N-linked glycosylation for CRT transport function [26] or for protein folding, maturation, stability, secretion and targeting to the plasma membrane [24,32]. If only the creatine transport efficiency of CRT were affected in glycosylation-deficient mutants, a comparable reduction in $V_{max}$ after enzymatic deglycosylation of surface proteins with PNGase F would be expected. However, our results showed only a reduction of 49 % in $V_{max}$ for PNGase F-deglycosylated CRT-NN cells. Thus the additional reduction of $V_{max}$ observed with the three glycosylation-deficient mutants must be the result of a lower density of mutant CRT in the plasma membrane compared with wild type CRT-NN. Indeed, densitometric and immunofluorescence evaluations showed an approx. 2–3-fold lower abundance of mutant CRT at the cell surface, suggesting an at-least-2-fold lower capacity for creatine transport of the partially or non-glycosylated form as compared with fully glycosylated CRT. Taken together, these results indicate a dual function for N-linked glycans in CRT: first, they are used for correct trafficking of CRT to the plasma membrane, although partially or non-glycosylated CRT may not be absolutely excluded from the plasma membrane; secondly, removal of one or both glycans from the second extracellular loop of CRT impairs its transport efficiency for creatine by a factor of 2. Interestingly, removal of one glycosylation site had approximately the same effect as removal of both sites. Similar deviations between surface presence and uptake efficiency have been reported for comparable glycosylation-deficient mutants of the NET [34,35] and the DAT [26].

In conclusion, we established an expression system for epitope-tagged CRT expression in mammalian cells that allowed identification of the 58 kDa polypeptide species as the genuine plasma membrane CRT monomer. The expression system opens an avenue for future studies on CRT mutations causing neurodegenerative disorders [49]. Moreover, we found that N-glycosylation of CRT is important for both, CRT trafficking to the plasma membrane and for its transport function. These findings may also be true for close members of the transporter family, such as GAT and 5 HTT.

We thank Professor Dr Ari Helenius, Institute of Biochemistry, ETH Zurich, for helpful discussions and advice, as well as for generously giving the calnexin antibody. We thank Christian Zahnd, Institute of Biochemistry, University of Zurich, for carefully revising this manuscript. Dr Henry Hugues and Dr Olivier Braissant, CHUV Lausanne, Switzerland, are acknowledged for pointing out to us the LDS-PAGE system, and for revising the final version of the manuscript. Dr Dietbert Neumann and Dr Uwe Schlattner are acknowledged for helpful discussions. This work was supported by the SUK (Swiss University Commission), Cooperation project Heart Remodelling in Health and Disease (N.S.), and by the Swiss Society for Research of Muscle Diseases (T.W.).

## REFERENCES

1 Wallimann, T., Dolder, M., Schlattner, U., Eder, M., Hornemann, T., Kraft, T. and Stolz, M. (1998) Creatine kinase: an enzyme with a central role in cellular energy metabolism. Magma **6**, 116–119

2 Palacin, M., Estevez, R., Bertran, J. and Zorzano, A. (1998) Molecular biology of mammalian plasma membrane amino acid transporters. Physiol. Rev. **78**, 969–1054

3 Malandro, M. S. and Kilberg, M. S. (1996) Molecular biology of mammalian amino acid transporters. Annu. Rev. Biochem. **65**, 305–336

4 Salomons, G. S., van Dooren, S. J., Verhoeven, N. M., Marsden, D., Schwartz, C., Cecil, K. M., DeGrauw, T. J. and Jakobs, C. (2003) X-linked creatine transporter defect: an overview. J. Inherit. Metab. Dis. **26**, 309–318

5 van der Knaap, M. S., Verhoeven, N. M., Maaswinkel-Mooij, P., Pouwels, P. J., Onkenhout, W., Peeters, E. A., Stockler-Ipsiroglu, S. and Jakobs, C. (2000) Mental retardation and behavioral problems as presenting signs of a creatine synthesis defect. Ann. Neurol. **47**, 540–543

6 Guerrero-Ontiveros, M. L. and Wallimann, T. (1998) Creatine supplementation in health and disease. Effects of chronic creatine ingestion *in vivo*: down-regulation of the expression of creatine transporter isoforms in skeletal muscle. Mol. Cell. Biochem. **184**, 427–437

7 Speer, O., Neukomm, L. J., Murphy, R. M., Zanolla, E., Schlattner, U., Henry, H., Snow, R. J. and Wallimann, T. (2004) Creatine transporters: a reappraisal. Mol. Cell. Biochem. **256–257**, 407–424

8 Neubauer, S., Remkes, H., Spindler, M., Horn, M., Wiesmann, F., Prestle, J., Walzel, B., Ertl, G., Hasenfuss, G. and Wallimann, T. (1999) Downregulation of the $Na^{(+)}$-creatine cotransporter in failing human myocardium and in experimental heart failure. Circulation **100**, 1847–1850

9 Murphy, R., McConell, G., Cameron-Smith, D., Watt, K., Ackland, L., Walzel, B., Wallimann, T. and Snow, R. (2001) Creatine transporter protein content localization, and gene expression in rat skeletal muscle. Am. J. Physiol. Cell. Physiol. **280**, C415–C4122

10 Tarnopolsky, M. A., Parshad, A., Walzel, B., Schlattner, U. and Wallimann, T. (2001) Creatine transporter and mitochondrial creatine kinase protein content in myopathies. Muscle Nerve **24**, 682–688

11 Walzel, B., Speer, O., Boehm, E., Kristiansen, S., Chan, S., Clarke, K., Magyar, J. P., Richter, E. A. and Wallimann, T. (2002) New creatine transporter assay and identification of distinct creatine transporter isoforms in muscle. Am. J. Physiol. Endocrinol. Metab. **283**, E390–E401

12 Walzel, B., Speer, O., Zanolla, E., Eriksson, O., Bernardi, P. and Wallimann, T. (2002) Novel mitochondrial creatine transport activity. Implications for intracellular creatine compartments and bioenergetics. J. Biol. Chem. **277**, 37503–37511

13 Peral, M. J., Garcia-Delgado, M., Calonge, M. L., Duran, J. M., De La Horra, M. C., Wallimann, T., Speer, O. and Ilundain, A. (2002) Human, rat and chicken small intestinal $Na^+$-$Cl^-$-creatine transporter: functional, molecular characterization and localization. J. Physiol. (Cambridge) **545**, 133–144

14 Schlattner, U., Mockli, N., Speer, O., Werner, S. and Wallimann, T. (2002) Creatine kinase and creatine transporter in normal, wounded, and diseased skin. J. Invest. Dermatol. **118**, 416–423

15 Murphy, R. M., Tunstall, R. J., Mehan, K. A., Cameron-Smith, D., McKenna, M. J., Spriet, L. L., Hargreaves, M. and Snow, R. J. (2003) Human skeletal muscle creatine transporter mRNA and protein expression in healthy, young males and females. Mol. Cell. Biochem. **244**, 151–157

16 Tarnopolsky, M., Parise, G., Fu, M. H., Brose, A., Parshad, A., Speer, O. and Wallimann, T. (2003) Acute and moderate-term creatine monohydrate supplementation does not affect creatine transporter mRNA or protein content in either young or elderly humans. Mol. Cell. Biochem. **244**, 159–166

17 Boehm, E., Chan, S., Monfared, M., Wallimann, T., Clarke, K. and Neubauer, S. (2003) Creatine transporter activity and content in the rat heart supplemented by and depleted of creatine. Am. J. Physiol. Endocrinol. Metab. **284**, E399–E406

18 West, M., Park, D., Dodd, J. R., Kistler, J. and Christie, D. L. (2005) Purification and characterization of the creatine transporter expressed at high levels in HEK-293 cells. Protein Expr. Purif. **41**, 393–401

19 Dodd, J. R., Zheng, T. and Christie, D. L. (1999) Creatine accumulation and exchange by HEK293 cells stably expressing high levels of a creatine transporter. Biochim. Biophys. Acta **1472**, 128–136

20 Kekelidze, T., Khait, I., Togliatti, A. and Holtzman, D. (2000) Brain creatine kinase and creatine transporter proteins in normal and creatine-treated rabbit pups. Dev. Neurosci. **22**, 437–443

21 Tran, T. T., Dai, W. and Sarkar, H. K. (2000) Cyclosporin A inhibits creatine uptake by altering surface expression of the creatine transporter. J. Biol. Chem. **275**, 35708–35714

22 Dodd, J. R. and Christie, D. L. (2001) Cysteine 144 in the third transmembrane domain of the creatine transporter is located close to a substrate-binding site, J. Biol. Chem. **276**, 46983–46988

23 Bennett, E. R. and Kanner, B. I. (1997) The membrane topology of GAT-1, a ($Na^+Cl^-$)-coupled gamma-aminobutyric acid transporter from rat brain. J. Biol. Chem. **272**, 1203–1210

24 Tate, C. G. and Blakely, R. D. (1994) The effect of N-linked glycosylation on activity of the $Na^+$- and $Cl^-$-dependent serotonin transporter expressed using recombinant baculovirus in insect cells. J. Biol. Chem. **269**, 26303–26310

25 Melikian, H. E., McDonald, J. K., Gu, H., Rudnick, G., Moore, K. R. and Blakely, R. D. (1994) Human norepinephrine transporter. Biosynthetic studies using a site-directed polyclonal antibody. J. Biol. Chem. **269**, 12290–12297

26 Li, L. B., Chen, N., Ramamoorthy, S., Chi, L., Cui, X. N., Wang, L. C. and Reith, M. E. (2004) The role of N-glycosylation in function and surface trafficking of the human dopamine transporter. J. Biol. Chem. **279**, 21012–21020

27 Hammond, C. and Helenius, A. (1995) Quality control in the secretory pathway. Curr. Opin. Cell. Biol. **7**, 523–529

28 Hurtley, S. M., Bole, D. G., Hoover-Litty, H., Helenius, A. and Copeland, C. S. (1989) Interactions of misfolded influenza virus hemagglutinin with binding protein (BiP). J. Cell. Biol. **108**, 2117–2126

29 Hurtley, S. M. and Helenius, A. (1989) Protein oligomerization in the endoplasmic reticulum. Annu. Rev. Cell Biol. **5**, 277–307

30 Braakman, I., Hoover-Litty, H., Wagner, K. R. and Helenius, A. (1991) Folding of influenza hemagglutinin in the endoplasmic reticulum. J. Cell Biol. **114**, 401–411

31 Gething, M. J. and Sambrook, J. (1992) Protein folding in the cell. Nature (London) **355**, 33–45

32 Torres, G. E., Carneiro, A., Seamans, K., Fiorentini, C., Sweeney, A., Yao, W. D. and Caron, M. G. (2003) Oligomerization and trafficking of the human dopamine transporter. Mutational analysis identifies critical domains important for the functional expression of the transporter. J. Biol. Chem. **278**, 2731–2739

33 Liu, Y., Eckstein-Ludwig, U., Fei, J. and Schwarz, W. (1998) Effect of mutation of glycosylation sites on the $Na^+$ dependence of steady-state and transient currents generated by the neuronal GABA transporter. Biochim. Biophys. Acta **1415**, 246–254

34 Melikian, H. E., Ramamoorthy, S., Tate, C. G. and Blakely, R. D. (1996) Inability to N-glycosylate the human norepinephrine transporter reduces protein stability, surface trafficking, and transport activity but not ligand recognition. Mol. Pharmacol. **50**, 266–276

35 Nguyen, T. T. and Amara, S. G. (1996) N-linked oligosaccharides are required for cell surface expression of the norepinephrine transporter but do not influence substrate or inhibitor recognition. J. Neurochem. **67**, 645–655

36 Guimbal, C. and Kilimann, M. W. (1993) A $Na^+$-dependent creatine transporter in rabbit brain, muscle, heart, and kidney. cDNA cloning and functional expression. J. Biol. Chem. **268**, 8418–8421

37 Lange, S., Auerbach, D., McLoughlin, P., Perriard, E., Schafer, B. W., Perriard, J. C. and Ehler, E. (2002) Subcellular targeting of metabolic enzymes to titin in heart muscle may be mediated by DRAL/FHL-2. J. Cell Sci. **115**, 4925–4936


Received 26 May 2005/30 August 2005; accepted 19 September 2005
Published as BJ Immediate Publication 19 September 2005, doi:10.1042/BJ20050857


38 Richards, M. L. and Sadee, W. (1986) Human neuroblastoma cell lines as models of catechol uptake. Brain Res. **384**, 132–137

39 Kilic, F. and Rudnick, G. (2000) Oligomerization of serotonin transporter and its functional consequences. Proc. Natl. Acad. Sci. U.S.A. **97**, 3106–3111

40 Ozaslan, D., Wang, S., Ahmed, B. A., Kocabas, A. M., McCastlain, J. C., Bene, A. and Kilic, F. (2003) Glycosyl modification facilitates homo- and hetero-oligomerization of the serotonin transporter. A specific role for sialic acid residues. J. Biol. Chem. **278**, 43991–40000

41 Daniels, G. M. and Amara, S. G. (1999) Regulated trafficking of the human dopamine transporter. Clathrin-mediated internalization and lysosomal degradation in response to phorbol esters. J. Biol. Chem. **274**, 35794–35801

42 Dodd, J. R. and Christie, D. L. (2005) Substituted-cysteine accessibility of the third transmembrane domain of the creatine transporter: defining a transport pathway. J. Biol. Chem. **280**, 32649–32654

43 Tosco, M., Faelli, A., Sironi, C., Gastaldi, G. and Orsenigo, M. N. (2004) A creatine transporter is operative at the brush border level of the rat jejunal enterocyte. J. Membr. Biol. **202**, 85–95

44 Nakashima, T., Tomi, M., Katayama, K., Tachikawa, M., Watanabe, M., Terasaki, T. and Hosoya, K. (2004) Blood-to-retina transport of creatine via creatine transporter (CRT) at the rat inner blood-retinal barrier. J. Neurochem. **89**, 1454–1461

45 Nash, S. R., Giros, B., Kingsmore, S. F., Rochelle, J. M., Suter, S. T., Gregor, P., Seldin, M. F. and Caron, M. G. (1994) Cloning, pharmacological characterization, and genomic localization of the human creatine transporter. Receptors Channels **2**, 165–174

46 Dai, W., Vinnakota, S., Qian, X., Kunze, D. L. and Sarkar, H. K. (1999) Molecular characterization of the human CRT-1 creatine transporter expressed in Xenopus oocytes. Arch. Biochem. Biophys. **361**, 75–84

47 Schloss, P., Mayser, W. and Betz, H. (1994) The putative rat choline transporter CHOT1 transports creatine and is highly expressed in neural and muscle-rich tissues. Biochem. Biophys. Res. Commun. **198**, 637–645

48 Saltarelli, M. D., Bauman, A. L., Moore, K. R., Bradley, C. C. and Blakely, R. D. (1996) Expression of the rat brain creatine transporter *in situ* and in transfected HeLa cells. Dev. Neurosci. **18**, 524–534

49 Rosenberg, E. H., Almeida, L. S., Kleefstra, T., deGrauw, R. S., Yntema, H. G., Bahi, N., Moraine, C., Ropers, H. H., Fryns, J. P., deGrauw, T. J. et al. (2004) High prevalence of SLC6A8 deficiency in X-linked mental retardation. Am. J. Hum. Genet. **75**, 97–105